nm^{-1} (Park Scientific)]. Images were obtained in the constant-force mode with filters off, an integral gain of 3.0, a proportional gain of 7.0, and a look-ahead gain of 0.0. The "d" scan head was used, which has a maximum scan range of 12 μm by 12 μm by 4.4 μm. The scan rate of the tip during image acquisition ranged from 25 to 60 Hz, and the applied tip-sample force was maintained at $F_{tip} \leq 10$ nN in solution. The AFM experiments were performed in aqueous solutions with a fluid cell (Digital Instruments) consisting of a quartz body with ports for fluid entry and exit. Large single crystals of HT, about 10 to 20 μm in diameter, were allowed to adsorb from a water suspension onto a freshly cleaved mica substrate. The samples were then removed from the suspension and dried at 120°C for 1 hour. The mica substrate was then attached to a magnetic stainless steel AFM sample disk. We positioned the AFM tip above single HT crystals, using an optical microscope, before imaging.

13. The hexagonal symmetry and the lattice constant $a' = 6.2$ Å are also evident from Fourier analysis of the AFM data.
14. S. A. C. Gould, K. Burke, P. K. Hansma, *Phys. Rev. B* **40**, 5363 (1989).
15. J. Ganaes, H. Lindgreen, P. L. Hansen, S. A. C. Gould, P. K. Hansma, *Ultramicroscopy* **42–44**, 1428 (1992).
16. H. Hartman *et al.*, *Clays Clay Miner.* **38**, 337 (1990).
17. G. W. Brindley and S. Kikkawa, *Am. Mineral.* **64**, 836 (1979).
18. C. L. Serna, J. L. Rendon, J. E. Iglesias, *Clays Clay Miner.* **30**, 180 (1982).
19. J. P. Thiel, C. K. Chiang, K. R. Poeppelmeier, *Chem. Mater.* **5**, 297 (1993).
20. M. C. Gastuche, G. Brown, M. M. Mortland, *Clay Miner.* **7**, 177 (1967); I. Pausch, H. H. Lohse, K. Schurmann, R. Allmann, *Clays Clay Miner.* **34**, 507 (1986).
21. G. Brown and M. C. Gastuche, *Clay Miner.* **7**, 193 (1967).
22. S. Budavari, Ed., *Merck Index* (Merck, Rahway, NJ, ed. 11, 1989), p. 1419.
23. The feasibility of using AFM to visualize, in situ, organic adsorbates was demonstrated for *tert*-butanol and *tert*-butylammonium cations on zeolite surfaces [A. L. Weisenhorn *et al.*, *Science* **247**, 1330 (1990)].
24. S. W. Carr, K. R. Franklin, C. C. Nunn, J. J. Pasternak, I. Scott, European patent 557,089 (1993).
25. J. M. Knox, J. Guin, E. G. Cockerell, *J. Invest. Dermatol.* **29**, 435 (1957); J. M. Knox, A. C. Griffin, R. E. Hakim, *ibid.* **32**, 51 (1960).
26. The pK_a values listed for MBSA in this report were determined by the titration of 1.6 mmol of MBSA in aqueous solution with NaOH.
27. The absorption of $MBSA^{1-}$ and $MBSA^{2-}$ on HT has been verified by several independent analyses. X-ray photoelectron spectroscopy reveals the presence of MBSA in amounts approximating those expected for monolayer coverages. Infrared spectra indicate the presence of $MBSA^{1-}$ or $MBSA^{2-}$ on HT, which is infrared-transparent between 1000 and 1300 cm^{-1}. Adsorption was also confirmed from the depletion of $MBSA^{1-}$ or $MBSA^{2-}$ from solutions to which HT had been added.
28. We optimized the MBSA structure depicted in Fig. 4 using MOPAC and the CAChE molecular modeling program. The optimized structure compares favorably with that determined from single-crystal x-ray diffraction of guanidinium 5-benzoyl-4-hydroxy-2-methoxybenzenesulfonate (V. A. Russell and M. D. Ward, in preparation). The infrared spectral features of MBSA anions on HT in the region between 1000 and 1300 cm^{-1} are nearly identical to those observed for the guanidinium salt of $MBSA^{1-}$ in which the sulfonate group is hydrogen-bonded to guanidinium protons and resides in a site of threefold C_{3v} symmetry. This arrangement is identical to that observed for a series of guanidinium sulfonates [V. A. Russell, M. C. Etter, M. D. Ward, *J. Am. Chem. Soc.* **116**, 1941 (1994)].
29. The . . . ABAB . . . pattern is also evident from Fourier analysis of the AFM data, which reveals two reciprocal space components along the reciprocal lattice vector a^* at 0.06 Å^{-1} and 0.12 Å^{-1}, consistent with the supercell depicted in Fig. 5C.
30. The coverages and orientation surmised from the AFM data, for both $MBSA^{1-}$ and $MBSA^{2-}$ adsorbates, are in agreement with previously reported chemical analyses and x-ray diffraction data of fully intercalated materials (*24*). Intercalation of $MBSA^{1-}$ and $MBSA^{2-}$ into the nitrate form of HT results in the expansion of the HT layers and the interatomic spacings of 21 and 13 Å, respectively. These values are consistent with the vertical orientation of the MBSA molecule, which has a height of about 11 Å. The larger interatomic spacing for $MBSA^{1-}$ can be attributed to bilayer packing in which interdigitation of $MBSA^{1-}$ ions on opposing HT layers is prohibited by the dense packing of the organic molecules. In contrast, the lower coverage of the $MBSA^{2-}$ ions permits interdigitation of opposing adsorbate layers, leading to a smaller interatomic spacing.
31. L. Ingram and H. F. W. Taylor, *Mineral. Mag.* **26** (no. 280), 465 (1967).
32. L. Addadi *et al.*, *Agnew. Chem.* **23**, 346 (1985); E. M. Landau, M. Levanon, L. Leiserowitz, M. Lahav, J. Sagiv, *Nature* **318**, 353 (1985); E. M. Landau *et al.*, *Pure. Appl. Chem.* **61**, 673 (1989); P. W. Carter and M. D. Ward, *J. Am. Chem. Soc.* **115**, 11521 (1993).
33. H.C. thanks Y. Liu and S. Yang for assistance in AFM imaging. This research was supported by the National Science Foundation and the Center for Interfacial Engineering at the University of Minnesota. M.D.W. also received support from the National Science Foundation and the Office of Naval Research. The work of A.C.H. was supported under an Upjohn Fellowship during 1992–1993.

30 June 1994; accepted 28 September 1994

Wolves, Moose, and Tree Rings on Isle Royale

B. E. McLaren* and R. O. Peterson

Investigation of tree growth in Isle Royale National Park in Michigan revealed the influence of herbivores and carnivores on plants in an intimately linked food chain. Plant growth rates were regulated by cycles in animal density and responded to annual changes in primary productivity only when released from herbivory by wolf predation. Isle Royale's dendrochronology complements a rich literature on food chain control in aquatic systems, which often supports a trophic cascade model. This study provides evidence of top-down control in a forested ecosystem.

Terrestrial food chains of length three—plants, herbivores, and carnivores—are found throughout the temperate zone of the Northern Hemisphere, yet their establishment, pervasiveness, and stability are enigmatic subjects of debate among community ecologists (*1*). According to one hypothesis, depletion of green plants by herbivores occurs only in exceptional circumstances because carnivores usually control herbivores (*2*). However, systems in which increases in the density of a species at one trophic level accompany increases at higher, dependent trophic levels support a counterargument (*3*). The top-down (trophic cascade) model predicts that changes in density at one trophic level are caused by opposite changes in the next higher trophic level and that such inverse correlations cascade down a food chain. Accordingly, effects such as changes in primary productivity (the energy flow to plants) become noticeable only when higher, masking trophic levels are removed. After removal of carnivores from a three-level system, the control of density relationships is passed down the chain, to herbivores. The bottom-up model predicts that positive correlations occur between density changes at all trophic levels and especially between adjacent trophic levels, that changes in primary productivity affect higher trophic levels, and that extinction of the top trophic level does not change density patterns in lower levels.

We investigated food chain control in a large mammal system through observation of three trophic levels—a living system that is unlike two-level models of ungulate dynamics, which simulate the herbivore-plant interaction but are insensitive to parameter changes in a carnivore equation (*4*), and is also unlike models for ungulates that ignore the effects of vegetation change (*5*). Tree-ring analyses were used to characterize the interaction between an herbivore population and its winter forage in a system with an apparent cycle between predator and prey: the wolves (*Canis lupus*) and moose (*Alces alces*) in Isle Royale National Park, Michigan, the largest island (544 km^2) in Lake Superior (*6*, *7*). Ring width in balsam fir (*Abies balsamea*), a tree that makes up 59% of winter moose diet (*8*), provided an index of the herbivore food base, even though it is not optimal forage for moose. We assumed that the annual wood accrual for fir was proportional to its foliar biomass, which is an approximate measure of standing forage crop.

Balsam fir covers a large area of Isle Royale (Fig. 1), although its relative abundance in the overstory has declined since the arrival of moose early in the 1900s, from 46% in 1848, to 13% in 1978, to ~5% today (*9*). The decline is attributed to the effect of moose herbivory; forests on small nearby islands that are less accessible to moose still have a large fir component (*10*). The lon-

Michigan Technological University, School of Forestry and Wood Products, Houghton, MI 49931, USA.

*To whom correspondence should be addressed.

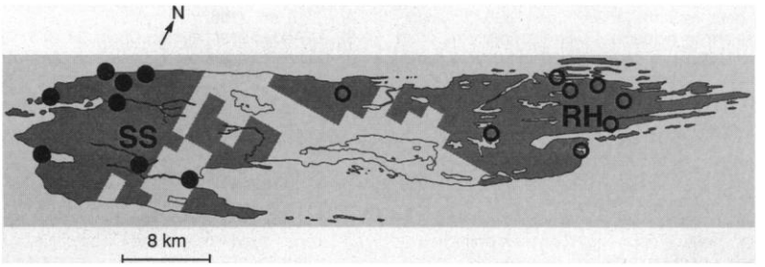

Fig. 1. Isle Royale National Park, showing the location of sampled balsam fir trees. Samples were collected randomly from intersection points of township grid lines within two broad regions of high understory fir density (shaded area) (*25*). Filled circles represent the locations of west-end trees, collected from a more established forest with a larger hardwood component; open circles represent east-end trees, collected from boreal forests that were burned extensively in 19th-century fires. The two regions are separated by a deciduous forest that originated from an extensive fire in 1936 and by upland hardwood forest at higher elevations. The locations of two other sample sites are marked RH, Rock Harbor, and SS, Siskiwit Swamp.

Table 1. Correlated annual changes in primary productivity and ring-width indices for balsam fir. The AET column shows the direction of change in AET (*24*) between a census year and the previous year (Fig. 3E). The RH and SS columns show the number of trees [out of 10 in the RH sample and 9 in the SS sample (Fig. 4)] for which the difference in ring width for these 2 years is in the same direction. Whereas ring-width release from 1979 to 1983 in the RH sample has no correlation with annual climate fluctuations, in the interval from 1984 to 1990, annual ring growth more closely tracks climate.

Year	AET	RH	SS
1979	−	3	2
1980	+	10	5
1981	−	0	3
1982	+	8	3
1983	−	1	3
1984	+	10	7
1985	+	8	6
1986	−	7	7
1987	−	8	7
1988	−	9	6
1989	+	8	2
1990	+	8	2
1991	−	10	5

gevity of fir in the understory and its large contribution to moose diet on Isle Royale facilitated the present study (*11*). Moreover, balsam fir exhibits an intriguing response to moose herbivory on Isle Royale, where areas of extreme suppression of fir growth on the west end of the island contrast with little-affected areas on the east end (*12*) (Fig. 2). We believe that the general response of fir is comparable to that of other forage species on Isle Royale.

The Isle Royale food chain appears to be a tightly linked, three-trophic-level system dominated by top-down control (Fig. 3). Over three decades, balsam fir trees from widely separated areas of the island displayed cyclic intervals of ring growth suppression that accompanied elevated moose densities. Annual variation in ring width during suppression was very low and did not show any correlation with a climate series calculated for Isle Royale, which contradicts earlier proposals that variation in natural populations arises from the physical systems that surround them (*13*).

A common harmonic pattern of period 16 to 18 years in east- and west-end tree-ring chronologies (*14*) echoed similar periodicity in the moose population (*15*). However, minima in the foliar biomass of understory balsam fir lagged behind moose population maxima by 1 to 2 years at the west end of the island and by 5 years at the east end (*16*). That these two populations of fir should be out of phase in their response to herbivore density changes was actually consistent with the prediction of classical predator-prey models, given plant populations with unequal intrinsic rates of increase (*17*). The west-end hardwood forest has usually had higher actual evapotranspiration (AET) associated with warmer, early summer temperatures than has the east-end boreal forest

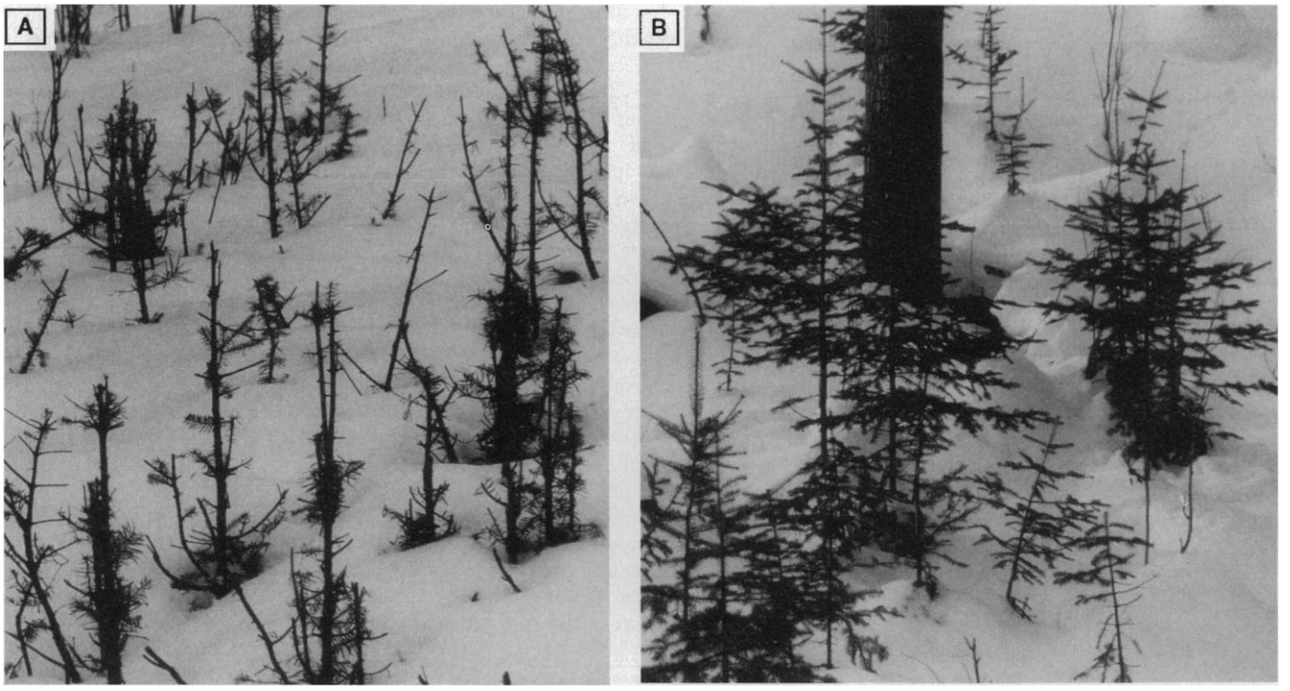

Fig. 2. Patterns of balsam fir growth suppression (**A**) and release (**B**) are evident throughout Isle Royale (*12*). We explain the difference in terms of herbivory and forest disturbance processes.

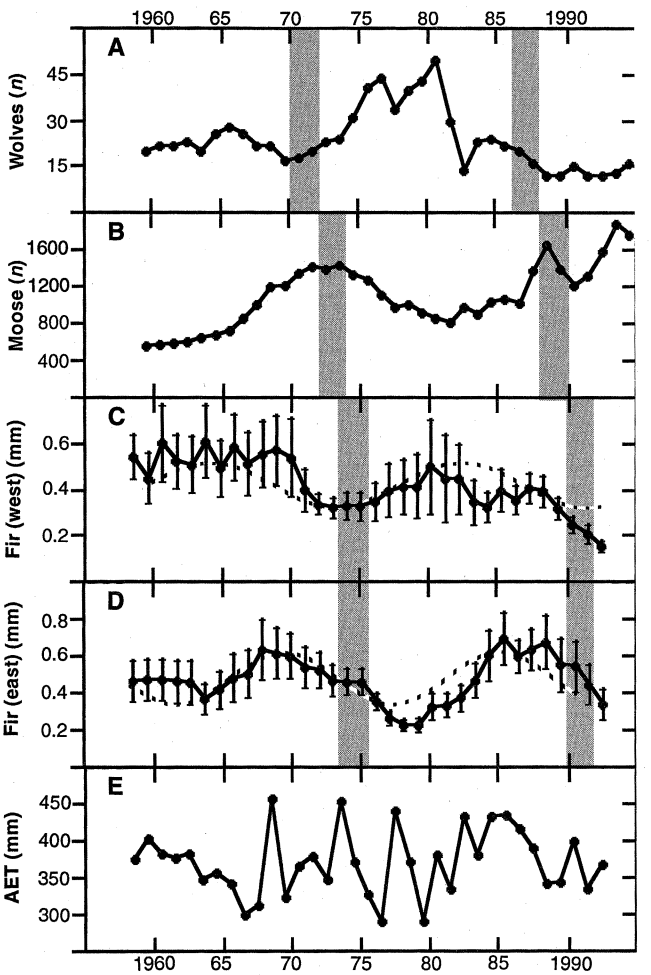

Fig. 3. The trophic system on Isle Royale, reconstructed for 1958 to 1994. (**A**) The number of wolves on the island from winter aerial counts. (**B**) Moose population size, reconstructed from collected skeletal remains (1959 to 1981) and from winter aerial counts (1982 to 1994). (**C**) Mean ring-width index (*26*) for eight balsam fir trees sampled in 1992 from the west end of Isle Royale (Fig. 1). Vertical bars are ±1 SEM from the arithmetic mean. Dashed line is the best-fit harmonic function (*14*). (**D**) Mean ring-width index for eight trees from the east end of the island, as in (C). (**E**) Actual evapotranspiration from April to October, calculated for a weather station about 20 km from Isle Royale. The AET is the amount of water available to plants during the growing season as a function of both rainfall and temperature and has a close relation to primary productivity (*24*). The shaded areas highlight intervals of forage suppression that we believe are closely tied to periods of elevated moose density, which in turn follow periods of low wolf density (note the lags between trophic levels). These intervals have no correspondence to AET.

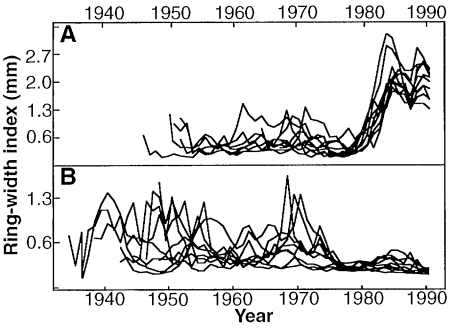

Fig. 4. Individual ring-width chronologies (*26*) for balsam fir trees collected from Isle Royale in 1992. (**A**) Ten trees, 26 to 48 years of age, from location RH (Fig. 1), in which fir height exceeded the reach of moose (3 m) in the late 1970s. (**B**) Nine trees, 48 to 60 years of age, from location SS (Fig. 1), for which total height at the time of sampling ranged from 1.08 to 1.57 m.

(*18*); consequently, we expected higher plant growth rates on the west end of Isle Royale.

Herbivore density, in turn, was largely determined by predation. The wolf population has fluctuated with changes in the number of moose older than 9 years in the prey population, prompting consequent changes in herbivore density by influencing calf survival rates (*6*, *7*, *19*). When old moose (and wolves) were relatively scarce, calf survival was high and moose numbers grew, which then led to depletion of balsam fir forage. Subsequent decline in the moose population was closely linked to wolf increase, itself fueled by aging of the moose population. Vegetation response followed moose response (Fig. 3), so it was not directly responsible for herbivore fluctuations. In summary, because wolf maxima precede moose minima, and moose maxima are similarly followed by fir minima, and because the vegetation dynamics appear to be more intimately linked to the wolf-moose interaction than to seasonal weather patterns, we believe that we have evidence for top-down control in a nonaquatic three-trophic-level system (*20*).

A strong supporting argument presents itself in the recent wolf decline on Isle Royale, when the wolf population reached an unprecedented low (*21*). The moose population accordingly reached a new, very high level, accompanied by strong suppression of balsam fir growth, in 1988 to 1991. This was especially apparent in the west-end sample (Fig. 3C). Without the context of a three-trophic-level interaction, fir decline and recovery cannot be explained; however, current disintegration of the system into a two-trophic-level interaction establishes even lower minima for fir growth than the suppressed level of the 1970s, which is more in agreement with the top-down than the bottom-up model.

Nevertheless, release of balsam fir from herbivory by moose does occur on Isle Royale when large-scale forest disturbances allow bottom-up influences to prevail. Additional samples of balsam fir showed extremes in the outcome of the herbivore-plant interaction and helped explain the broadly contrasting pattern of suppression on the two ends of the island (Figs. 2 and 3). An east-end subsample of trees (RH), collected from an open-canopy area of past forest disturbance, increased in growth after a period of high wolf predation of moose in the late 1970s. A west-end subsample (SS), collected from a closed-canopy hardwood forest heavily browsed by moose, showed increasingly suppressed growth, particularly in the current decade of high moose density (Fig. 4). This high suppression accompanies lower fir density in many similar areas on the west end; such a pattern may explain the more tightly coupled cycle between moose and fir there. Whereas ring-width patterns before 1980 were coordinated in both samples and matched those in the extensive samples (for example, release in the 1960s, suppression in the late 1970s), the recent period of release, especially in the RH sample, was immediately associated with closer correlation with the primary productivity index (Table 1). Thus, only when moose density was relatively low, which allows the link to the wolf-moose interaction to be removed or weakened by disturbance, did understory balsam fir grow in a fashion consistent with the bottom-up model. We believe that external processes such as fire and large windstorms can override usual top-down effects in a forest, but that this effect occurs primarily when the density of the next higher trophic level is low.

The uniqueness of the Isle Royale study is that it complements studies of top-down effects in aquatic systems (*1*). The establishment of bottom-up control in a terrestrial system when higher trophic levels are removed also parallels results from aquatic studies (*22*) and follows analogous predictions for ungulate populations without predators (*5*). Furthermore, this study supports the top-down argument that was originally applied to the Isle Royale system (*23*).

REFERENCES AND NOTES

1. M. D. Hunger and P. W. Price, *Ecology* **73**, 724 (1992).

2. N. G. Hairston, F. E. Smith, L. B. Slobodkin, *Am. Nat.* **94**, 421 (1960).
3. S. L. Pimm, *The Balance of Nature* (Univ. of Chicago Press, Chicago, IL, 1992), chap. 14.
4. We considered the model in G. Caughley, *Analysis of Vertebrate Populations* (Wiley, New York, 1977), pp. 130–132.
5. A. T. Bergerud, *Trends Ecol. Evol.* **3**, 68 (1988); *Can. J. Zool.* **64**, 1515 (1986).
6. R. O. Peterson, R. E. Page, K. M. Dodge, *Science* **224**, 1350 (1984).
7. R. O. Peterson and R. E. Page, *J. Mammal.* **69**, 89 (1988); *Acta Zool. Fenn.* **174**, 251 (1983).
8. K. L. Risenhoover, thesis, Michigan Technological University (1987), p. 49.
9. R. A. Janke, D. McKaig, R. Raymond, *For. Sci.* **24**, 115 (1978); B. E. McLaren, unpublished data (figures are for the west end of Isle Royale).
10. J. D. Snyder and R. A. Janke, *Am. Midl. Nat.* **95**, 79 (1976).
11. Suppression of balsam fir growth on Isle Royale by moose foraging occurs because of continuous removal of upper branches in winter. Trees remain alive in the forest understory for several decades, because lateral branches are protected from browsing by snow cover and because balsam fir is tolerant of shade. Trees in this study (except those represented in Fig. 4A) ranged from 34 to 68 years of age but came from a consistent height interval of 1 to 3 m at the time of sampling. The age variation made no contribution to variation in growth rates.
12. T. A. Brandner, R. O. Peterson, K. L. Risenhoover, *Ecology* **71**, 155 (1991).
13. G. Caughley and A. Gunn, *Oikos* **67**, 47 (1993); S. L. Pimm and A. Redfearn, *Nature* **334**, 613 (1984); M. H. Williamson, *The Analysis of Biological Populations* (Arnold, London, 1982), chap. 5.
14. A harmonic function fitted with an ordinary least squares approach, period 17.8 years, matched the west-end chronology with $R^2 = 0.38$; a function with period 16.1 years matched the east-end chronology with $R^2 = 0.70$. Following M. G. Bulmer [*J. Anim. Ecol.* **43**, 701 (1978)], functions incorporating both a harmonic term and a first-order autoregressive term were matched to the series, with improved fits of $R^2 = 0.68$ and $R^2 = 0.81$, respectively.
15. The cycle period inferred from empirical consideration of the three-trophic-level system is shorter than a period cited earlier, which was derived from a body-mass regression (*6*). However, the confidence interval for the allometric equation also included the shorter period of 16 to 18 years.
16. Ring-width suppression followed height-growth suppression in both samples by about 3 years.
17. G. Caughley, *Oecologia* **54**, 309 (1976). The plant with the inferior growth rate lags behind herbivore density more than does the plant with the superior growth rate.
18. B. E. McLaren, unpublished data; R. M. Linn, thesis, Duke University (1957).
19. R. O. Peterson, unpublished data.
20. Our result is new primarily because studies of long-term processes in terrestrial food chains are rare, especially studies of those in which top carnivores still exist. A. R. E. Sinclair and colleagues [*Am. Nat.* **141**, 173 (1993)] recently described the well-known snowshoe hare (*Lepus americana*) cycle in the Yukon Territory, Canada, as generating cyclic suppression of white spruce (*Picea glauca*). These authors, however, favored an explanation in meteorological driving forces. Other studies [for example, L. B. Keith, A. W. Todd, C. J. Brand, R. S. Adamcik, D. H. Rusch, *Int. Congr. Game Biol.* **13**, 151 (1976); L. B. Keith and L. A. Windberg, *Wildl. Monogr.* **58**, 70 (1978)] have considered plant-herbivore and herbivore-carnivore relations for the snowshoe hare, but in different study areas. The third trophic level in the fox-prey system studied by E. R. Lindström and colleagues [*Ecology* **75**, 1042 (1994)] was a parasite.
21. J. M. Thurber and R. O. Peterson, *J. Mammal.* **74**, 879 (1993).
22. D. J. McQueen, M. R. S. Johannes, J. R. Post, T. J. Stewart, D. R. S. Lean, *Ecol. Monogr.* **59**, 289 (1989); S. R. Carpenter *et al.*, *Ecology* **68**, 1863 (1987); M. Lynch and J. Shapiro, *Limnol. Oceanogr.* **26**, 86 (1981); J. L. Brooks and S. I. Dodson, *Science* **150**, 28 (1965).
23. L. Oksanen, S. D. Fretwell, J. Arruda, P. Niemela, *Am. Nat.* **118**, 240 (1981); for other contrasting published ideas concerning predator-prey cycles on Isle Royale, see (*6*) and J. Pastor and R. J. Naiman, *Am. Nat.* **139**, 690 (1992).
24. M. L. Rosenzweig, *Am. Nat.* **102**, 67 (1968). The index was calculated with the use of daily records from Thunder Bay, Ontario.
25. Understory fir density exceeds 250 ha^{-1} over about 70% of Isle Royale's land area and exceeds 10,000 ha^{-1} in many shoreline forests. Values were obtained by averaging density estimates for stems ≤2 m in 0.01-ha plots at the corners of each (square-mile) township section.
26. The ring-width index is the ratio of increments calculated as a summation of volume differences for a series of stacked conic sections representing the stems of sampled trees, divided by the cambial surface area at the beginning of each growing season for each year. An aggregate index, comprising ring-width measurements ($\pm 10^{-2}$ mm) averaged for four radii at 5- to 10-cm increments along stems, is presented. This intensity of sampling permits an accurate height-growth reconstruction of the trees and measurement of the wood volume increment throughout the trees' stems.
27. We acknowledge the National Park Service (NPS) for permission to sample trees; V. G. Smith, University of Toronto, for the design of the ring-width index; R. J. Miller, Ontario Ministry of Natural Resources, for the development of analytic software and loan of measurement equipment; Environment Canada for supplying weather records; and the following for financial support: National Geographic Society, NPS Earthwatch, the Boone and Crockett Club, and NSF grant DEB-9317401. W. C. Kerfoot and F. H. Wagner kindly reviewed this manuscript and offered many helpful suggestions.

13 May 1994; accepted 6 September 1994

Requirement for Intron-Encoded U22 Small Nucleolar RNA in 18S Ribosomal RNA Maturation

Kazimierz T. Tycowski, Mei-Di Shu, Joan A. Steitz*

The nucleoli of vertebrate cells contain a number of small RNAs that are generated by the processing of intron fragments of protein-coding gene transcripts. The host gene (*UHG*) for intron-encoded human U22 is unusual in that it specifies a polyadenylated but apparently noncoding RNA. Depletion of U22 from *Xenopus* oocytes by oligonucleotide-directed ribonuclease H targeting prevented the processing of 18S ribosomal RNA (rRNA) at both ends. The appearance of 18S rRNA was restored by injection of in vitro–synthesized U22 RNA. These results identify a cellular function for an intron-encoded small RNA.

The nucleolus is the site of rRNA synthesis, processing, and assembly into ribosomes (*1*). In vertebrate cells, rRNA is transcribed as a 40 to 47S precursor that is subsequently cleaved at multiple sites to yield the mature 18S, 28S, and 5.8S rRNAs. The nucleolus also contains small nucleolar ribonucleoproteins (snoRNPs), each composed of a short RNA, known as snoRNA, and at least one protein (*2*). On the basis of their mode of synthesis, vertebrate snoRNAs of the U series fall into two classes. U3, U8, and U13 RNAs are transcribed as independent units by RNA polymerase II and carry 5′-trimethylguanosine caps (*3*). In contrast, snoRNAs U14 through U21 are all encoded within introns of genes for abundantly expressed proteins. They mature by intron processing mechanisms, as yet poorly defined, and possess monophosphates at their 5′ ends (*2*). Most snoRNAs are associated with a conserved nucleolar antigen, fibrillarin (*2*, *3*).

Several snoRNPs have been shown to function in rRNA processing (*2*). The most abundant, U3, is essential for cleavage within the 5′ external transcribed spacer (ETS) of both vertebrate (*4*, *5*) and yeast (*6*) precursor rRNAs (pre-rRNAs) and may contribute to 18S and 5.8S rRNA formation as well (*6*, *7*). Yeast U14, which is not intron-encoded, and snR30 (small nuclear RNA 30) are required for cell viability and accumulation of 18S rRNA (*8*), whereas yeast ribonuclease (RNase) MRP is essential for 5.8S rRNA maturation (*9*) and snR10 enhances growth and processing of the 35S pre-rRNA (*10*). *Xenopus* U8 is the only snoRNA found to function in vertebrate 28S and 5.8S rRNA processing (*11*).

Human RNA Y (*3*), now renamed U22, is a fibrillarin-associated snoRNA that contains a 5′-monophosphate and has the potential to form a terminal stem-loop-stem motif with conserved boxes C and D (*12*). We completed sequence analysis of human U22 RNA and also determined the nucleotide sequence of two (A and B) *Xenopus* U22 genes that differ only at positions 28 and 41 (Fig. 1A). Human and *Xenopus* U22 RNAs are ~75% identical, with the identities confined mostly to the termini and a middle section of the molecule. Neither shows significant homology to other known RNAs.

Southern (DNA) blot analysis of genomic DNA detected a single locus for human U22 (*13*), another feature that distinguishes

Howard Hughes Medical Institute, Department of Molecular Biophysics and Biochemistry, Yale University School of Medicine, 295 Congress Avenue, New Haven, CT 06536, USA.

*To whom correspondence should be addressed.